

## Machine learning potential for accurate radiation defect simulations in bcc-Fe

Sehyeok Park and Takuji Oda\*

Department of Nuclear Engineering, Seoul National University, 1, Gwanak-ro, Gwanak-gu, Seoul 151-744, Republic of Korea

\*Corresponding author: oda@snu.ac.kr

### 1. Introduction

Radiation damage in nuclear materials has been studied for many decades using experiment and computer simulation. However, it is difficult to investigate collision dynamics by experiment due to the small space and short time in which each collision cascade process occurs [1]. In the experiment, only defects that survived and developed through various thermal processes such as migration, recovery and clustering can be observed, and the details of the primary radiation damage processes cannot be known.

Therefore, various computational methods have been used to simulate the primary radiation damage processes, such as Binary Collision Approximation (BCA), Kinetic Monte Carlo (KMC), and Molecular Dynamics (MD) [2]. Among them, classical MD (CMD) has been widely used [3,4] because it can deal with the system size and time scales required for the simulation of primary damage processes in detail. However, the previous studies [5,6] show that the threshold displacement energy (TDE) and cascade damage simulations by CMD are greatly dependent on the potential model.

In bcc-Fe, which is important as the base material of ferritic/martensitic steels, the C15 type cluster is highly stable unlike other bcc metals [7]. The energy landscape of C15 clusters is very complicated due to the involvement of a larger number of vacancies and self-interstitial atoms (SIAs) than the parallel-dumbbell cluster with the same cluster size (Fig. 1). This complicated energy landscape makes hard to correctly simulate the stability of C15 clusters with existing embedded atom method (EAM) potentials.

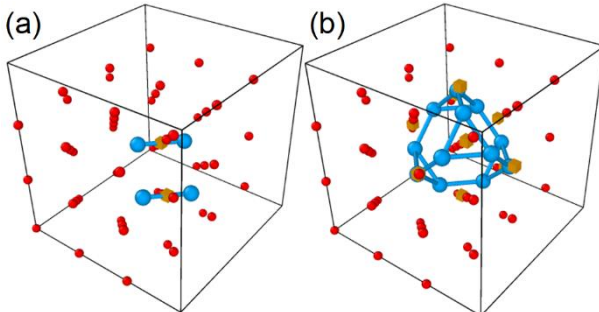


Fig. 1. Structure of interstitial cluster in bcc lattice with cluster size 2. The atoms in perfect crystal position are marked by red spheres, SIAs by blue spheres, and vacancies by orange cubes. (a) parallel dumbbells aligned in the  $\langle 111 \rangle$  direction. The cluster consists of 4

SIAs and 2 vacancies. (b) C15 type cluster. The cluster consists of 12 SIAs and 10 vacancies.

In the present study, we develop a potential model that accurately reproduces the stability of various radiation defects including C15 in bcc-Fe at a reasonably low calculation cost, aiming to realize high-precision radiation damage CMD simulations in the future. To obtain accuracy beyond that of existing EAM models, the moment tensor potential (MTP) [8], a type of machine learning potential, was adopted.

### 2. Methods

#### 2.1. Reference data by DFT calculation

In general, a machine learning potential model is constructed in reference to energy, force and stress data obtained by first-principles calculations. Thus, we need to first prepare the reference data set to reproduce the defect-related properties. For this aim, density functional theory (DFT) calculations with  $3 \times 3 \times 3$  and  $4 \times 4 \times 4$  supercells containing 54 and 128 atoms, respectively, were performed. The energy, force and stress data of 1257 configurations were gathered and used to construct an MTP model. Table 1 lists the reference data configurations classified into seven types. All DFT calculations were performed using Vienna *ab initio* simulation package (VASP) [9] with the projector augmented-wave (PAW) method [10]. The Perdew-Burke-Ernzerhof (PBE) exchange correlation functional [11] was utilized. The semi-core potential with 14 valence electrons ( $\text{Mg}3p^64s^13d^7$ ) was used. The  $4 \times 4 \times 4$  and  $3 \times 3 \times 3$  Monkhorst-Pack grid k-point samplings were used for  $3 \times 3 \times 3$  and  $4 \times 4 \times 4$  supercells, respectively.

Table 1. Details of each reference data.  $N_{traj}$  is the number of trajectories/configurations, and  $N_{atom}$  is the number of atoms for each system.

System type	$N_{traj}$	$N_{atom}$	Type	Temp. [K]
Perfect	370	54	Dynamic	300-2100
Isotropic Deformation	100	54	Static	-
Shear Deformation	50	54	Static	-
Defects (SIA, Vac, Fixed Vol.)	480	45-59, 130	Dynamic	300, 600, 1000

	127		Static	-
Defects (SIA, Vac. Relaxed Vol.)	30		Static	-
Defect Migration	80	53-55	Static	-
Liquid	20	54	Static	-
<b>Total</b>	1257			

## 2.2. MTP model construction

An MTP model [8] was constructed using the energy, force and stress data prepared by the DFT calculation as the fitting target. MTP uses polynomial basis functions for the radial component and tensor-form basis functions for the angular component. The size of basis functions is controlled by a single parameter called *level*. Increasing the *level* is expected to increase the accuracy of the MTP model, but at a higher calculation cost. Based on the results of several test calculations, we set *level* to 16. The minimum and maximum cutoff radii for the radial basis functions were 0.59 and 6.0 Å, respectively.

We constructed four types of MTP models using different sets of reference data. The PM1 was constructed using default reference data with  $3 \times 3 \times 3$  supercells. PM2 and PM3 were constructed including relaxed SIA cluster structures and relaxed vacancy cluster structures, respectively. PM4 additionally includes a C15 cluster structure with  $4 \times 4 \times 4$  supercells to improve the description in the C15 cluster. The number of reference configurations for each PM is 1218 for PM1, 1236 for PM2, 1254 for PM3, and 1257 for PM4, respectively.

In the training of MTP, fitting parameters are randomly initialized and optimized by an iteration method. Thus, each MTP gives different fitting quality and potential model performance depending on the initial parameters. In this study, for each PM type, we selected a representative MTP model from those constructed with four different initial parameters based on the fitting RMS error and the defect formation energy.

## 2.2. Details of performance test

For the model performance test, we calculated several material properties, such as lattice constant, elastic constants, and defect energies. All CMD simulations were performed using the Large-scale Atomic/Molecular Massively Parallel Simulator (LAMMPS) code [12]. The defect formation energy and the potential energy change in static displacement simulation, in which only one atom is displaced toward a neighboring atom, were calculated with  $3 \times 3 \times 3$  supercells ( $54 \pm 1$  atoms). These results were compared with DFT calculation results. The defect cluster stability was calculated with  $30 \times 30 \times 30$  supercells ( $54000 + \alpha$  atoms) and compared with the DFT results with 1024 atoms after the correction of the system-size effect [13]. For comparison with previous

potential models, the EAM model developed by Ackland et al [14], which is noted as AM04, was used.

## 3. Results and discussion

### 3.1. Fitting quality

The RMSEs in energy/force/stress from the DFT calculation for constructed MTP models are presented in Table 2. Good agreement with DFT is observed.

Table 2. RMSEs from the DFT calculation for four MTP models.

	PM1	PM2	PM3	PM4
Energy (meV/atom)	5.261	4.967	5.647	5.564
Force (eV/Å)	0.112	0.105	0.107	0.099
Stress (GPa)	0.691	0.684	0.789	0.691

### 3.2. Material properties

The results of the performance test on the lattice constant, bulk modulus, and point defect formation energies are shown in Table 2. The MTP models reasonably reproduce the DFT results for all quantities. As seen in the improved agreement with DFT from PM1 to PM4, the accuracy of the defect formation energy was enhanced by the additional defect data.

For defect cluster stability, Fig. 2 shows the defect formation energy differences between C15 and  $\langle 111 \rangle$  parallel-dumbbell clusters calculated by the MTP models in the range of 2-6 cluster size. For example, for cluster size 4, the C15 cluster is composed of 18 SIAs and 14 vacancies, while the  $\langle 111 \rangle$  parallel-dumbbell cluster is 8 SIAs and 4 vacancies. The results are compared with DFT and AM04. The MTP models show better agreement with DFT than AM04. The residual errors in the MTP models are considered to stem from the fact that large clusters were not included in the MTP training reference in the present study. To be specific, we included only 2-5 cluster sizes for  $\langle 111 \rangle$  parallel cluster and 2-4 cluster sizes for the C15 cluster. The previous study by DFT calculation [7] predicts that the direction of the dumbbell defect in parallel cluster changes from  $\langle 110 \rangle$  dumbbell to  $\langle 111 \rangle$  dumbbell in more than the cluster size 5. The MTP may not have properly explained the change in the dumbbell direction. Another reason for residual errors is the difference in supercell size between DFT and MTP. A cluster of defects in a bulk crystal induces a long-range elastic field. This causes some errors in the calculation of parallel-dumbbell defect clusters even with the correction of the system size effect [13]. And although the effect of the system size on the C15 cluster was not systematically studied in the previous study, it can be expected that the error of the C15 cluster will be larger than that of the parallel cluster when considering the elastic field by extra defects involved in the C15 cluster.

A static displacement test with  $\langle 135 \rangle$  direction displacement is presented in Fig. 3.  $\langle 135 \rangle$  is a crystallographically open direction. The MTP models outperform AM04, and show good agreement with the DFT up to about 1.4 Å of displacement. The poor performance at short distances is reasonable because the reference data for short distances were not prepared. If this MTP is to be used in collision cascade simulations, the short-range interaction needs to be modified, such as by connecting to the ZBL screened Coulomb interaction potential. The performance of MTP in collision cascade simulations will be investigated in the future.

Table 3. Material properties obtained by DFT calculation and CMD calculations with four MTP models.  $a$  is lattice constant, and  $K$  is bulk modulus.

	DFT	PM1	PM2	PM3	PM4
$a$ (Å)	2.83	2.84	2.84	2.84	2.84
$K$ (GPa)	192	181	167	169	174
Defect formation energy (eV)					
Vacancy	2.16	2.11	2.09	2.10	2.15
SIA $\langle 110 \rangle$	4.43	4.5	4.39	4.43	4.39
SIA $\langle 111 \rangle$	5.25	4.9	5.02	5.33	5.24

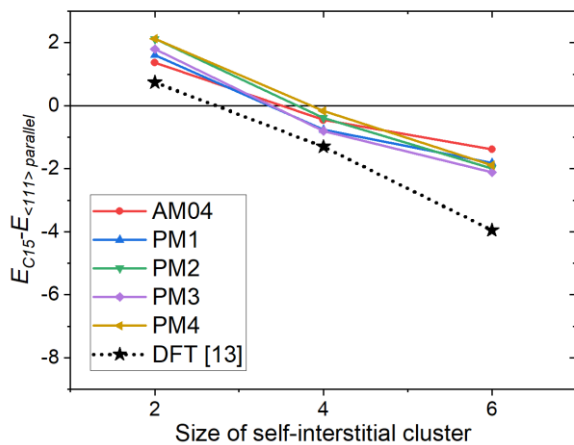


Fig. 2. Defect cluster formation energy difference between C15 and the parallel-dumbbell configurations. The parallel-dumbbell configuration with  $\langle 110 \rangle$  dumbbell up to 4 SIAs and  $\langle 111 \rangle$  dumbbell at larger cluster size are selected as the lowest energy defect configuration for parallel-dumbbell clusters.

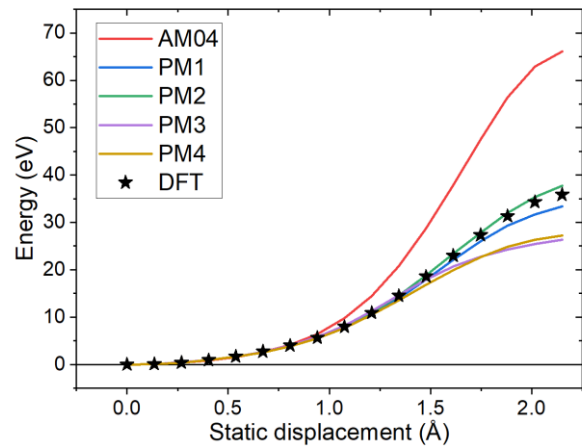


Fig. 3. Potential energy curves obtained by static displacement calculations along  $\langle 135 \rangle$  direction.

#### 4. Conclusion

In this study, MTP models of  $\alpha$ -Fe were constructed by referring to the energy, force, and stress data calculated by DFT. The constructed MTP models reasonably agree with DFT reference data. In addition, we confirmed that the MTPs reasonably reproduce lattice constant, bulk modulus, and defect formation energies as well as the defect cluster stability and the potential energy change by a static displacement. These results show improved performance compared to the previous EAM potential.

In future work, we will adjust the short-range interaction for a better description of collision cascade dynamics by adding specific potential energy data for short ranges.

#### 5. Acknowledgement

This research was supported by the National Research Foundation of Korea (NRF) grant funded by the Korean government (MSIT) (No. 2018R1C1B6007879; No. 2021M2D6A1048220), the Brain Korea 21 FOUR Program (No. 419990314119), and the Creative-Pioneering Researchers Program through Seoul National University.

#### REFERENCES

- [1] D.J. Bacon, T. Diaz de la Rubia, Molecular dynamics computer simulations of displacement cascades in metals, *J. Nucl. Mater.* 216 (1994) 275–290. [https://doi.org/10.1016/0022-3115\(94\)90016-7](https://doi.org/10.1016/0022-3115(94)90016-7).
- [2] K. Nordlund, Historical review of computer simulation of radiation effects in materials, *J. Nucl. Mater.* 520 (2019) 273–295. <https://doi.org/10.1016/j.jnucmat.2019.04.028>.
- [3] T.D. de la Rubia, W.J. Phythian, Molecular dynamics studies of defect production and clustering in energetic displacement cascades in copper, *J. Nucl.*

- Mater. 191–194, P (1992) 108–115.  
[https://doi.org/10.1016/S0022-3115\(09\)80017-2](https://doi.org/10.1016/S0022-3115(09)80017-2).
- [4] L. Malerba, M.C. Marinica, N. Anento, C. Björkas, H. Nguyen, C. Domain, F. Djurabekova, P. Olsson, K. Nordlund, A. Serra, D. Terentyev, F. Willaime, C.S. Becquart, Comparison of empirical interatomic potentials for iron applied to radiation damage studies, *J. Nucl. Mater.* 406 (2010) 19–38.  
<https://doi.org/10.1016/j.jnucmat.2010.05.017>.
- [5] S. Park, M.J. Banisalman, T. Oda, Characterization and quantification of numerical errors in threshold displacement energy calculated by molecular dynamics in bcc-Fe, *Comput. Mater. Sci.* 170 (2019) 109189.  
<https://doi.org/10.1016/j.commatsci.2019.109189>.
- [6] C. Björkas, K. Nordlund, Comparative study of cascade damage in Fe simulated with recent potentials, *Nucl. Instruments Methods Phys. Res. Sect. B Beam Interact. with Mater. Atoms.* 259 (2007) 853–860.  
<https://doi.org/10.1016/j.nimb.2007.03.076>.
- [7] F. Willaime, C.C. Fu, M.C. Marinica, J. Dalla Torre, Stability and mobility of self-interstitials and small interstitial clusters in  $\alpha$ -iron: ab initio and empirical potential calculations, *Nucl. Instruments Methods Phys. Res. Sect. B Beam Interact. with Mater. Atoms.* 228 (2005) 92–99.  
<https://doi.org/10.1016/j.nimb.2004.10.028>.
- [8] I.S. Novikov, K. Gubaev, E. V Podryabinkin, A. V Shapeev, The MLIP package: moment tensor potentials with MPI and active learning, *Mach. Learn. Sci. Technol.* 2 (2021) 025002.  
<https://doi.org/10.1088/2632-2153/abc9fe>.
- [9] G. Kresse, J. Hafner, Ab initio molecular dynamics for liquid metals, *Phys. Rev. B.* 47 (1993) 558–561.  
<https://doi.org/10.1103/PhysRevB.47.558>.
- [10] P.E. Blöchl, Projector augmented-wave method, *Phys. Rev. B.* 50 (1994) 17953–17979.  
<https://doi.org/10.1103/PhysRevB.50.17953>.
- [11] J.P. Perdew, K. Burke, M. Ernzerhof, Generalized Gradient Approximation Made Simple, *Phys. Rev. Lett.* 77 (1996) 3865–3868.  
<https://doi.org/10.1103/PhysRevLett.77.3865>.
- [12] S. Plimpton, Fast Parallel Algorithms for Short-Range Molecular Dynamics, *J. Comput. Phys.* 117 (1995) 1–19. <https://doi.org/10.1006/jcph.1995.1039>.
- [13] R. Alexander, M.-C. Marinica, L. Proville, F. Willaime, K. Arakawa, M.R. Gilbert, S.L. Dudarev, Ab initio scaling laws for the formation energy of nanosized interstitial defect clusters in iron, tungsten, and vanadium, *Phys. Rev. B.* 94 (2016) 024103.  
<https://doi.org/10.1103/PhysRevB.94.024103>.
- [14] G.J. Ackland, M.I. Mendeleev, D.J. Srolovitz, S. Han, A. V Barashev, Development of an interatomic potential for phosphorus impurities in  $\alpha$ -iron, *J. Phys. Condens. Matter.* 16 (2004) S2629–S2642.  
<https://doi.org/10.1088/0953-8984/16/27/003>.